

Characterization of the Optical Throughput Performance of the Navy Prototype Optical Interferometer (NPOI)

Xiaolei Zhang^a, J. Thomas Armstrong^a, James A. Clark III^a, G. Charmaine Gilbreath^a, Robert Lucke^a, Sergio Restaino^a, David Mozurkewich^b, James A. Benson^c, Donald J. Hutter^c, Nat White^d, Henrique Schmitt^e, Joshua P. Walton^e

^aNaval Research Laboratory, Remote Sensing Division, 4555 Overlook Ave. SW, Washington, DC 20375, USA;

^bSeabrook Engineering, 9310 Dubarry Ave., Seabrook, MD 20706, USA;

^cUS Naval Observatory Flagstaff Station, P.O. Box 1149, Flagstaff, AZ 86002-1149, USA;

^dLowell Observatory, 1400 W. Mars Hill Rd., Flagstaff, AZ 86001, USA;

^e Interferometrics Inc., Herndon, VA 20171, USA

ABSTRACT

We have developed an approach for systematically investigating the optical throughput performance of the different segments of a Michelson stellar interferometer, and applied it to the characterization of the Navy Prototype Optical Interferometer (NPOI). We report the results of the first phase of throughput measurements on NPOI, as well as some of the lessons learned.

Since the current generation of ground-based optical interferometers all suffers from varying degree of throughput degradation while the dominant causes for throughput loss are expected to vary for each individual instrument, the methodologies and approaches developed here could be of general use for the quantitative characterization of the throughput performance of the different optical interferometers, a prerequisite for its ultimate improvement.

Keywords: optical interferometry; optical throughput characterization

1. BACKGROUND

The Navy Prototype Optical Interferometer¹ is a 6-element, long-baseline stellar interferometer operating in the wavelength range of 450-850nm. The back-end beam combiner employs a mostly free-space hybrid combining scheme, with characteristics intermediate between pair-wise and all-in-one approaches.²

Various earlier attempts at characterizing the optical throughput of NPOI optical system using stellar photometry indicated that its value is in the range of 1-5%, which means that 95-99% of the visible photons received by the siderostats are lost somewhere during the light propagation path to reach the detector, with the blue end of the spectral bandpass suffering especially high throughput loss. This throughput performance, low as it may seem, is in fact not atypical for the current generation of ground-based optical interferometers, and in most of these cases a detailed and quantitative assessment of the major contributors to throughput loss are also lacking.

The throughput measurements conducted in the past on NPOI suffered from uncertainties of the afterpulsing characteristics of the avalanche photodiode (APD) used as detectors on the back-end beam combiner. Furthermore, none of the previous tests were conducted in a systematic and thorough manner. It is thus desirable to devise a new set of measurements aimed towards a thorough and quantitative assessment of the spectral throughput performance of the various segments of NPOI optical train, with results that are independent of the absolute gain factors of the detectors.

Send correspondence to Xiaolei Zhang, E-mail: xiaolei.zhang@tnrl.navy.mil, Telephone: 1 202 404 2389

Report Documentation Page

Form Approved
OMB No. 0704-0188

Public reporting burden for the collection of information is estimated to average 1 hour per response, including the time for reviewing instructions, searching existing data sources, gathering and maintaining the data needed, and completing and reviewing the collection of information. Send comments regarding this burden estimate or any other aspect of this collection of information, including suggestions for reducing this burden, to Washington Headquarters Services, Directorate for Information Operations and Reports, 1215 Jefferson Davis Highway, Suite 1204, Arlington VA 22202-4302. Respondents should be aware that notwithstanding any other provision of law, no person shall be subject to a penalty for failing to comply with a collection of information if it does not display a currently valid OMB control number.

1. REPORT DATE 2006		2. REPORT TYPE		3. DATES COVERED 00-00-2006 to 00-00-2006	
4. TITLE AND SUBTITLE Characterization of the Optical Throughput Performance of the Navy Prototype Optical Interferometer (NPOI)				5a. CONTRACT NUMBER	
				5b. GRANT NUMBER	
				5c. PROGRAM ELEMENT NUMBER	
6. AUTHOR(S)				5d. PROJECT NUMBER	
				5e. TASK NUMBER	
				5f. WORK UNIT NUMBER	
7. PERFORMING ORGANIZATION NAME(S) AND ADDRESS(ES) Naval Research Laboratory, Remote Sensing Division, 4555 Overlook Avenue SW, Washington, DC, 20375				8. PERFORMING ORGANIZATION REPORT NUMBER	
9. SPONSORING/MONITORING AGENCY NAME(S) AND ADDRESS(ES)				10. SPONSOR/MONITOR'S ACRONYM(S)	
				11. SPONSOR/MONITOR'S REPORT NUMBER(S)	
12. DISTRIBUTION/AVAILABILITY STATEMENT Approved for public release; distribution unlimited					
13. SUPPLEMENTARY NOTES					
14. ABSTRACT We have developed an approach for systematically investigating the optical throughput performance of the different segments of a Michelson stellar interferometer, and applied it to the characterization of the Navy Prototype Optical Interferometer (NPOI). We report the results of the first phase of throughput measurements on NPOI, as well as some of the lessons learned. Since the current generation of ground-based optical interferometers all suffers from varying degree of throughput degradation while the dominant causes for throughput loss are expected to vary for each individual instrument, the methodologies and approaches developed here could be of general use for the quantitative characterization of the throughput performance of the different optical interferometers, a prerequisite for its ultimate improvement.					
15. SUBJECT TERMS					
16. SECURITY CLASSIFICATION OF:			17. LIMITATION OF ABSTRACT	18. NUMBER OF PAGES	19a. NAME OF RESPONSIBLE PERSON
a. REPORT unclassified	b. ABSTRACT unclassified	c. THIS PAGE unclassified			

2. TEST APPROACHES

The new test approaches for throughput measurement are designed to allow the flexibility of probing the transmission properties of various segments of the NPOI optical train, while minimizing the impact on the existing optics.

For the probing beams, we choose to use the collimated beams originating from the artificial whitelight and laser sources currently residing on the back-end beam combiner table, which are routinely launched from the back-end toward the siderostats during normal observing to aid in the alignment procedure. Retroreflections are introduced at the different locations along the propagation paths in order to determine the differential transmission/throughput loss of the segment of optics under investigation.

The beams on the beam combiner table at different locations is brought out of the beam combiner table by a Newport beam-steering periscope assembly, which has relatively small footprint and can be inserted into the beam path to intercept and redirect the beam to the detection optics. The periscope also helps to raise the beam height so it can get out of the insulation on the sides of the beam combiner table. The periscope measurement locations are chosen so as not to block the outgoing beams from the artificial laser and whitelight sources on the beam combiner table, and thus were required to be near the vary end of the optical propagation paths, as will be described in details shortly.

The additional optics used for the throughput measurements are situated mostly on a stand-alone small optical table, or the so-called ScienceDesk by MellesGriot. It is passively vibration-isolated, and has castors which allow for easy relocation and can be locked down during data taking. The ScienceDesk used for our tests accommodates a 2.5'x3' breadboard.

On the ScienceDesk (c.f. Figures 1,2), a second periscope helps to lower the incoming beam height and redirects the beam to the two feed mirrors which together have enough degrees-of-freedom for maintaining the beam axis. A Newport broadband beam splitter splits the beam two paths. One path, which was idle during the whitelight measurements but feeds the laser light into the laser powermeter head through a focusing Fabry lens pair. The other path goes through a couple filterwheels (with neutral density and bandpass filters mounted) to a focusing lens which feeds the whitelight or laser signal onto the CCD camera. Having both the laser powermeter and CCD readouts during the laser throughout measurement provided additional sanity check on the linearity and precision of each detectors.

The Fabry lens pair in the laser powermeter path was originally intended to reduce the image movement on the laser powermeter head during the differential measurements. However, we later realized that this setup on makes the image spot stationary with respect to the angular directional changes of the incoming beam, whereas the lateral shift of the image spot is uncorrected. We thus used two additional targets along the beam path to verify the constancy of the optical axis each time we move to a new beam sampling location.

A stand-alone PC with monitor was used in the data acquisition. The computer has a PCI slot which takes in a National Instrument framegrabber card (NI PCI-1428) which is interfaced to the CCD camera, of model Adimec-1000m. The data acquisition for the CCD used custom software written based on National Instruments' LabWindows/CVI package. More details on the hardware and software systems for the throughput test can be found in Zhang (2006)³

The first phase of the throughput tests, conducted in August of 2005 and described in details below, were conducted at the NeHe laser frequency. Differential power readouts at the different locations along the beamline, of the retroreflected beams, allow the estimation of throughput loss of the corresponding optical segments at the HeNe wavelength (633nm). Monitoring of the output laser power level between the measurements are also performed to ensure the reliability of the differential measurements.

For all the tests conducted three different locations of the autocollimating mirrors are used: at the output of the beam combiner table; on the switchyard table after the beams have gone through the faster delay lines (FDLs); and at the siderostat (SID) mirrors. In the following we describe in details the different steps of the test.

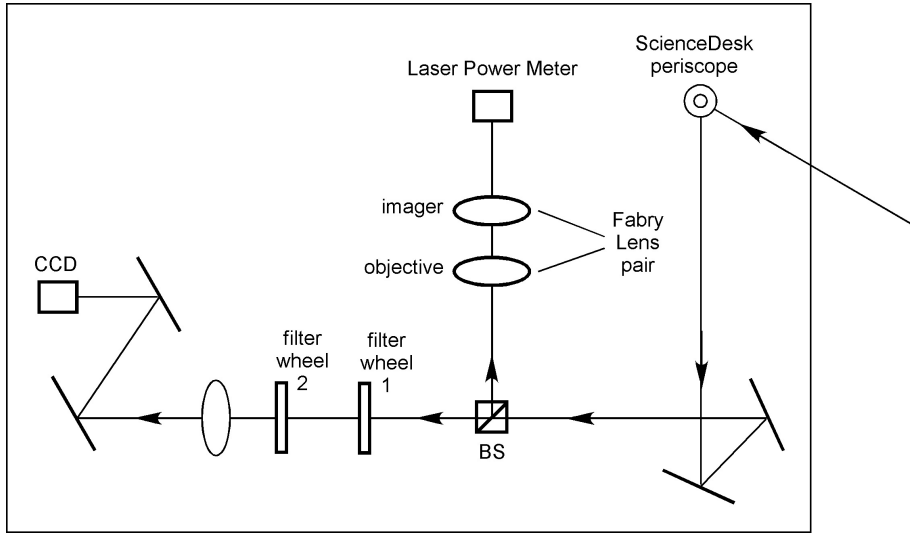


Figure 1. Schematics of the Optics on the ScienceDesk

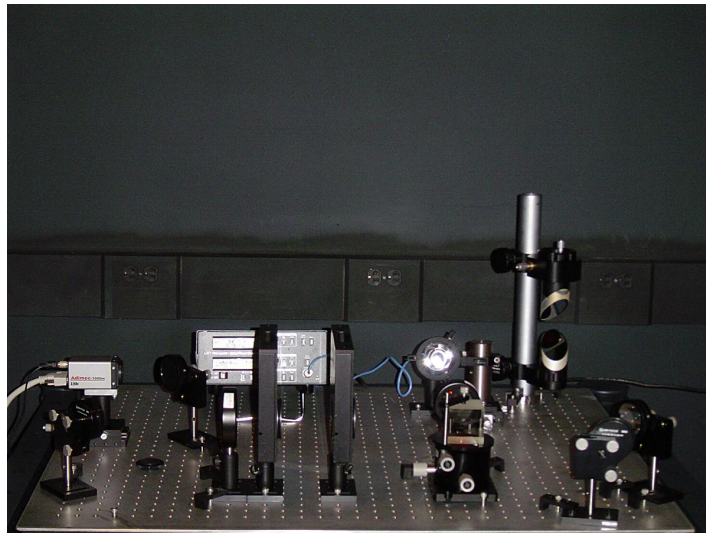


Figure 2. Completed Optics Assembly on the ScienceDesk

2.1. Characterizing the Throughput of the Spectrometer Injection Optics

In this step we set up the autocollimating mirrors at the output of the beam combiner as shown in Figure 3. The sampling locations 1,2,3 are the first ones where the retro-reflected beam, after going through double-pass propagation, can be sampled without blocking the outgoing beams. From here on the beams will experience only single pass, and the measurements locations 1-9 indicated on Figure 3 will allow us to characterize the throughput performance of the paraboloids, prisms, pinholes and achromat lenses.

At the converging or diverging locations of the beams a lens of varying focal lengths, either positive or negative, are used to recollimate the beam before being brought out of the beam combiner table.

Additional measurements can be obtained at marked location 10, with and without the pinhole in place, to directly assess the pinhole throughput issue and compare with the corresponding measurements using the lenses to recollimate the beam.

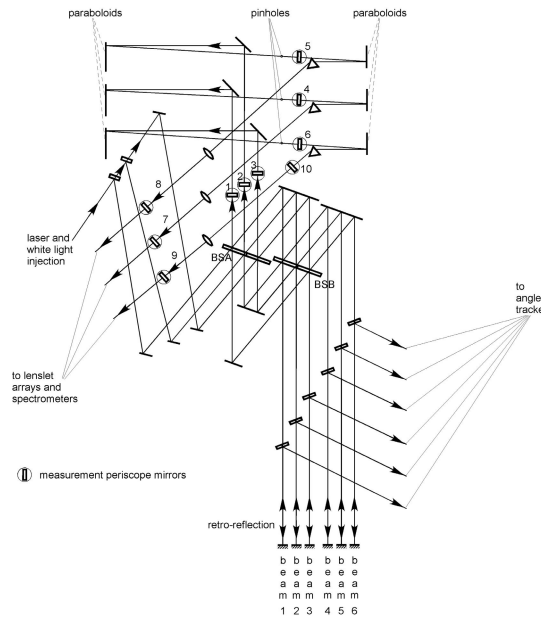


Figure 3. Optics on the NPOI Beam Combining Table. Also Shown Are Test Configurations for Characterizing the Throughput of the Spectrometer-Injections Optics

2.2. Characterizing the Throughput of the Fast Delay Lines (FDLs)

The loss due to the FDL propagation paths can be assessed by comparing the return signals measured on the beam combiner table, at locations as marked in Figure 4 for the respective beam lines, with the autocollimation mirror located first outside the beam combiner table, and subsequently in front of the FDL. While autocollimating in front of the FDLs, the delayline lengths can be varied to investigate the effect of propagation length on throughput, which reflects in part scattering losses due to small-scale irregularities of the mirror surfaces, as well as the effect of residual misalignment of the optics on throughput.

2.3. Characterizing the Throughput of the Feed System

Referring to Figure 5, taking the measurement at the location indicated by the periscope symbol with the siderostat (SID) mirror in the autocollimation mode, and comparing it with the corresponding measurement result of the previous step (autocollimation after the FDL and with the periscope at the same location), allow the assessment of the propagation loss of the front-end optics from the FDL to the SID mirror. Though only one measurement location is marked in this figure it is understood that the same measurement will be repeated for every beam line.

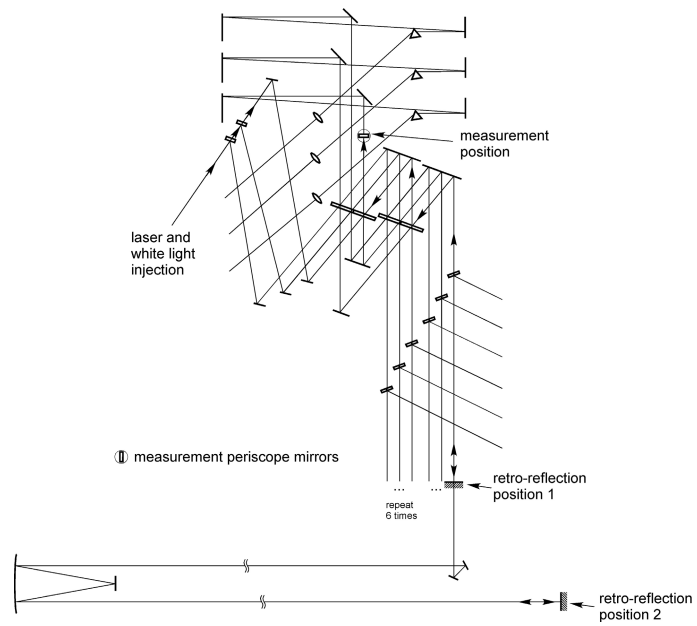


Figure 4. Test Configuration for Characterizing the Throughput of the Fast Delay Line (FDL) Paths

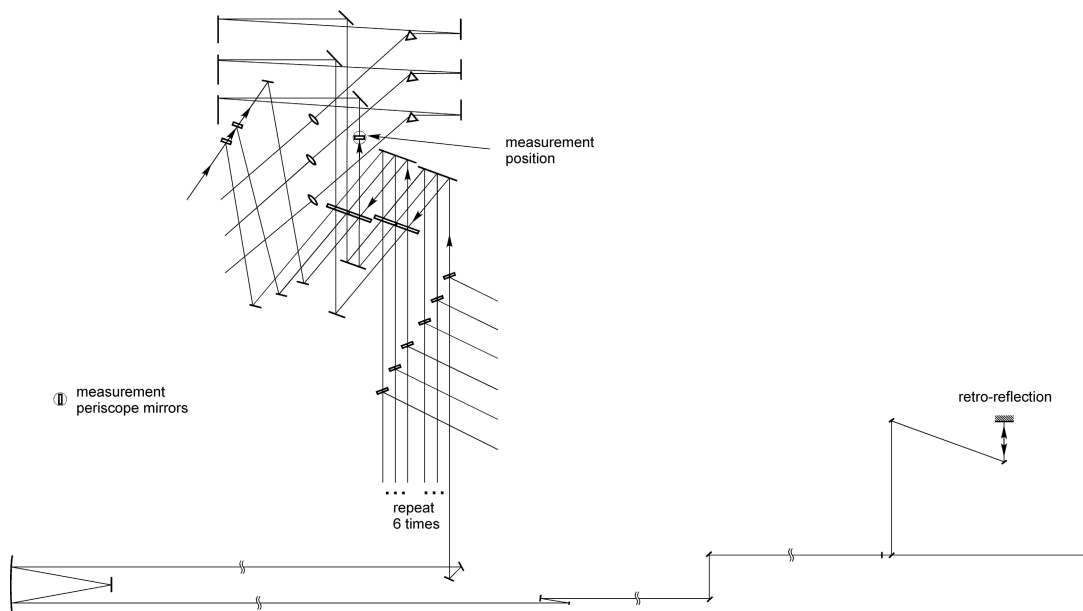


Figure 5. Test Configuration for Characterizing the Throughput of the Feed System

2.4. Characterizing the Throughput of the Fiber Injection and Propagation Paths

As indicated in Figure 6, in order to measure the throughput performance of the lenslet array and fiber propagation paths, in addition to the measured point at the input of the spectrometer, which is obtained in an earlier step (Figure 3, locations 7,8,9), we also need to disconnect the fiber connector leading to the avalanche photodiode (APD) detectors so as to obtain the output power at the end of this segment of the fiber. A custom multimode fiber from Fiberguide Industries of 50 feet in length is used to connect the fiber connector in the electronic room, and thread it through the mouse-hole on the wall and bring it into the inner room where the beam combiner resides, so the light can be channeled onto the ScienceDesk optics. This fiber is made by the same company which made our original fibers (also multimode), but the new fiber is of slightly larger core diameter than the existing ones used in the system, so all the light can be collected and channeled onto the measurement setup.

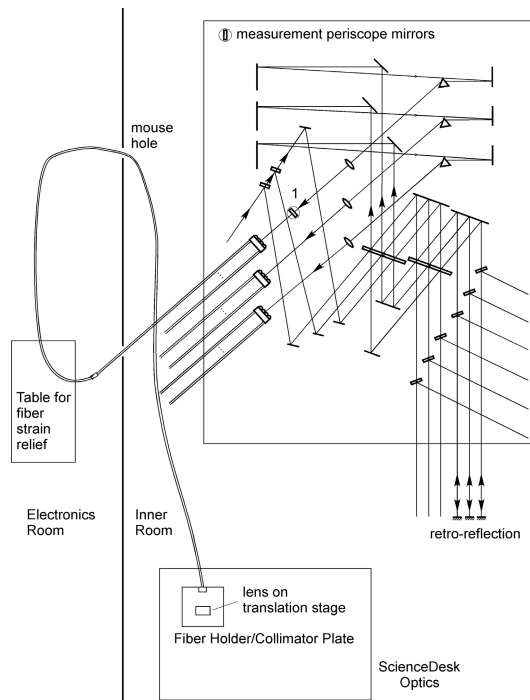


Figure 6. Test Configuration for Characterizing the Throughput of the Fiber Injection and Propagation Paths

A custom mount structure is made to hold the fiber holder which is mounted rigidly with respect to the lens holder used for collimating the output beam from the fiber, so it can be directed to the ScienceDesk input optics, bypassing however the ScienceDesk periscope.

During the tests, we have also manually scanned the laser input beam onto the lenslet array across all spectrometer channels and recorded the readout by embedded software system, in order to compare the relative throughput of all the channels of a spectrometer at the HeNe frequency. This step however does not give the spectral dependence of the fiber transmission, only the relative transmission of all channels at the laser frequency.

2.5. Characterizing the Throughput of the Beam Combining Optics

In order to characterize the performance of the science beam-splitters BSA and BSB, the beam splitters leading to the angle tracker, as well as some of the relay mirrors, the outgoing-beam power in single-pass should be measured at various accessible locations, as indicated in Figure 7. Throughput tests during previous years had arrived at some estimates of the losses for this segment of the propagation paths.

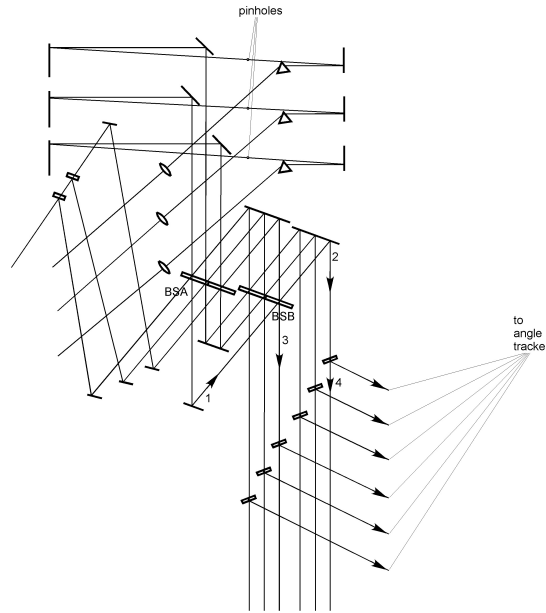


Figure 7. Test Configuration for Characterizing the Throughput of the Beam Combining Optics

3. RESULTS OF THE FIRST PHASE OF MEASUREMENTS

3.1. Overview of the Tests

The first phase of the throughput measurements of the NPOI optical train was conducted during the week of August 8, 2005. Due to time constraints as well as to the low flux of the existing whitelight source on the beam combiner table, only laser throughput measurements have been conducted. Whitelight, spectral throughput measurements using narrow-band filters are planned for the near future, likely using an intensified CCD to replace the current CCD camera. Further follow-on tests will include single-pass, absolute photometry and throughput measurements using stellar sources.

The week of August 8, being in the middle of the Monsoon season, did not allow the opening of the two imaging siderostat huts at night to do the feed system throughput measurement for these stations. We have only obtained the throughput measurements of the feed systems for the 4 astrometric stations since the SID mirrors for these four stations are located in closed domes, and the throughput measurements can be done during day time.

Partly due to the time constraint and partly to safety precautions, only one spectrometer path (that of spectrometer 3) and selected fiber/APD channels have been measured for throughput.

3.2. Characterizing the Fast Delay Lines (FDLs)

The throughputs of the Fast Delay Line (FDL) segments of the optical paths were obtained through the differential flux measurements in double-pass configurations (Figure 3) with the retroreflection introduced at the two located sandwiching the FDLs. We have performed this measurement for all six NPOI beams, and each differential measurement was performed once for delay line cart parked in the front-most location of the delayline track (corresponding to the shortest delay length), and once for delay line cart parked all the way back (corresponding to the longest delay). The double-pass difference in pathlengths between the two parking positions is about 35 meters.

When calculating the throughput values for each pair of “before” and “after” measurements, we have compared the results given by the laser powermeter differential measurements, and the CCD differential measurements. These are found to track each other fairly well – the throughput given by these two instruments are

usually within a couple percent if a short time average is made – for this particular set of measurements where both the “before” and the “after” beams are the 1.4 inch collimated beam. This agreement is impressive especially since the CCD is measuring flux at the image plane after the collimated beam is focusing by a lens, whereas the laser powermeter is effectively measuring the flux at the aperture/pupil plane since a Fabry lens pair has been used to re-image the pupil. The agreement between the two measurements shows that little flux is lost due to sidelobes not included in the CCD integration box.

Here is a summary of the throughput measurement results for the six delayline paths, and two parking positions for each path, obtained through an average of the laser and CCD results. Note that the numbers below have been converted to the equivalent single-pass throughput values by taking the square-root of the original double-pass values as given by the raw data, even though in actuality the the single-pass throughput may or may not be equal exactly to the square-root of the double-pass throughput, especially in the presence of path-length-dependent throughput loss:

- Delayline 1: Front: 0.83 Back: 0.76
- Delayline 2: Front: 0.82 Back: 0.73
- Delayline 3: Front: 0.85 Back: 0.82
- Delayline 4: Front: 0.86 Back: 0.84
- Delayline 5: Front: 0.80 Back: 0.73
- Delayline 6: Front: 0.86 Back: 0.80

The dependence of the measured throughput on the pathlength difference between the mirrors, as indicated by the different throughput values when the delayline cart is parked at the front or at the back, indicates that mirror reflectance loss is not the only contributor to the throughput loss, other factors such as scattering (due to small-scale roughness of the surface) and diffraction (due to wavefront curvature) may also have played a role. This is supported also by the fact that for the amount of throughput loss measured, and the number of double-pass reflections in the path (19 including the vacuum window surfaces), the average reflectance would have been 97% per surface to account for the measured throughput, whereas the mirrors themselves were originally specified to be 99.5% reflecting, though they might have degraded over the years.

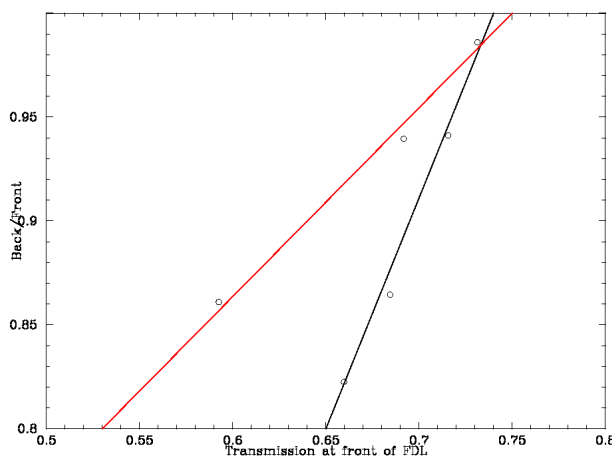


Figure 8. Possible correlation of the ratio of double-pass throughputs of the FDL path when the cart is parked at the front and at the back of the FDL, and the throughput when the cart is at the front of the FDL. The two lines drawn over the measured data points indicate two possible ways to fit the data.

Figure 8 plots the ratios of the delayline throughputs measured when the cart was parked at the front and at the back, versus the absolute throughput levels as represented by the throughput measured when the delayline was parked at the front. The data clustering in fact were better than indicated in the figure, as the range of display has been zoomed-in to show the difference. Possible causes of this dependence include the small-scale

surface roughness of the mirrors, and the roughness of the vacuum windows. Effectively this correlation shows that the surface roughness at the earlier part of a propagation path continues to exert an influence for the throughput degradation towards further propagation path.

3.3. Characterizing the Feed System

The feed system includes all the front-end optics prior to the FDL, i.e., the beam compressor optics, the periscope mirrors, the SID and NAT (narrow angle tracker) mirrors, and the vacuum pipe windows. The details of the measurement configuration is shown in Figure 4. The two retroreflection positions for the differential measurement are, first, off the SID mirrors themselves, and second, off the autocollimation mirrors at the input of the FDLs.

Due to the height of the periscope on the combiner table, the Celotex cover on the beam combiner table cannot be closed during the throughput measurements, and the background light in the room prevented NAT loop from locking. Manual fine-centroiding of the image had to be done each time just prior to each measurement readout. The short-time stability of the system is good enough for the image to remain in the integration box during the measurement period every time.

As in the case of the throughput measurements for the FDLs, for the feed system throughput characterization we once again have the 1.4 inch collimated beams to work with at the back-end for the two retroreflection positions (even though the beam at the front-end, before the beam compressor, was much larger). Thus we had once again achieved high measurement accuracy, with the throughputs measured by the laser power meter and the CCD usually agree within a few percent of each other, and the repeatability for measurements done at different times were excellent.

The throughputs of the four astrometric feed systems are measured as follows (here as well, we have converted the double-pass measurements to equivalent single-pass numbers by taking the square-root of the measured throughput. Averages have been taken of the respective laser- and CCD-measured throughputs):

Astrometric Center, on beam 2: 0.75
Astrometric East, on beam 3: 0.72
Astrometric West, on beam 4: 0.76
Astrometric North, on beam 6: 0.5

Here we can see that compared to the other three beamlines Astrometric North on beam 6 has abnormally low throughput. We have done visual inspections of the laser spot on the Astro North SID and repeated this measurement several times, and the measurement results appears to withstand.

The feed system propagation path is much longer than the FDL propagation path, and the number of reflections are even larger, yet the propagation loss for most of the beam lines is comparable to the FDL path. This perhaps has something to do with the oversized optics used for this segment of the optical path.

In Figure 9, a correlation of the throughput of the feedsystem with the differential throughput in the FDL path is indicated. If the correlation does correspond to a physical cause, it apparently continues the trend indicated in the FDL data that the roughness in the earlier part of the optics (i.e. FDL optics) continues to impact an influence towards later part of the optics (in this case the feed path). The correlation however is weak, and there are only three data points to determine this correlation apart from the one abnormal baseline. Additional data points in the future from the two imaging stations will help settle the issue.

3.4. Characterizing the Spectrometer Injection Optics on the Beam Combiner Table

The spectrometer injection optics contains optical elements such as the achromat, the two paraboloids surrounding the pinhole, the pinhole itself, the dispersing prism, and one fold mirror. The detailed configuration for this segment of the test is Figure 3. In the actual tests conducted in August 2005, we had combined the two-stage measurement plotted in Figure 3 into a single-stage overall throughput measurement during due mainly to time constraints.

The averaged throughput for this segment is 0.46 for spectrometer 3. This measurement is more uncertain than the FDL and feed system throughput measurements described before due to the fact that here beams of

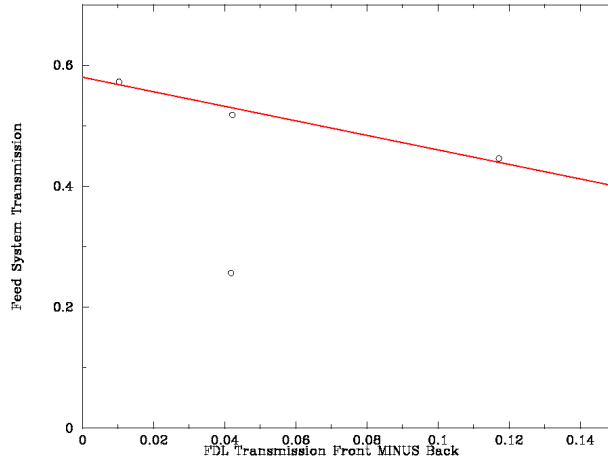


Figure 9. Possible correlation of the feed system throughput with the differential throughputs of the FDL path when the cart is parked at the front and at the back of the FDL. Throughputs plotted are double-pass values.

different sizes and collimating status are involved – one is the 1.4 inch collimated beam at the entrance of the beam combiner, and another is a converging beam at the input of the lenslet, which was further recollimated by a negative lens, forming a beam of roughly 0.5 cm diameter before being sent out to the ScienceDesk. Different-sized beams makes the laser power meter responses not being identical for the two differential measurements (since the different active regions in the laser power meter head has different sensitivity) – in fact we have to move the laser powerhead location and by-pass the Fabry lens pair for this set of measurements in order to better match the “before” and “after” beam sizes, but by doing this we lost the angular insensitivity which was enabled by the Fabry lens pair . The CCD measurements, on the other hand, is made uncertain by the uncertainty in the nominal values of the ND filters inserted.

It is to be noted that the throughput in this leg depends strongly on the alignment of the pinhole, and on the focusing of the system (as well as on seeing conditions in the case of stellar measurement). So this throughput number is expected to be variable and is more strongly alignment-dependent than the throughput values in other segments of the optical path. We have deferred the pinhole throughput measurement at location 10 in Figure 3 to the future tests.

3.5. Characterizing the Lenslet Array Injection and Fiber Throughput

The lenslet array injection and the first part of the fiber propagation path were originally suspected as a possible major contributor of the throughput loss. As it turned out, the measured transmission is quite reasonable. The configuration for this test is described in Figure 6. In what follows we quote only the measurement results from the CCD, since the laser power meter does not have the same sensitivity for the “before” and “after” cases since the beams in the two cases were of significantly different sizes after collimation and reimaging. For the CCD measurements, on the other hand, we were able to defocus the image on the camera for the lenslet array injection case so that it covers roughly the same area on the CCD as for the fiber-end image, and both have similar surface brightness as well, so no additional ND filter needed to be inserted, and the integration time on the CCD could thus be set the same.

We have corrected about 3% of transmission loss for the 50 ft test fiber (which has a core diameter of 400 μm compared to our existing fiber’s core diameter of 333 μm , thus can receive most of the photons being piped over), based on the manufacturer’s specification sheet. A direct measurement of the fiber loss was not successful since the segments of fibers we attach onto the end of the 50 ft, 400 μm diameter fiber are also of 400 μm diameter, and the insertion loss in this case dominated any propagation loss.

The transmission at the HeNe laser frequency for the four fiber channels on spectrometer 3 are found to be:

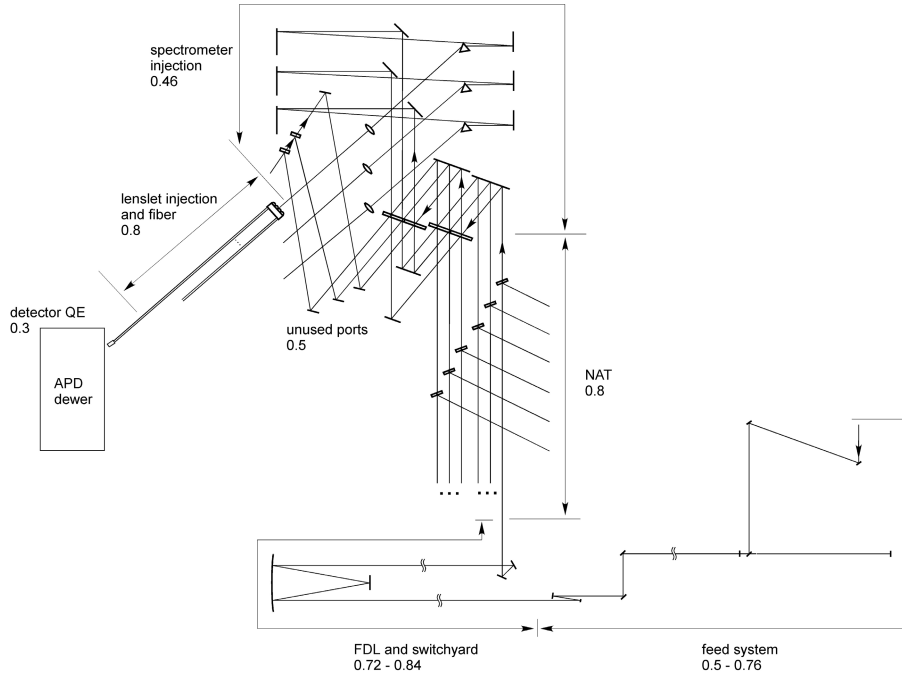


Figure 10. Overall System Throughput Breakup

- Channel 1 of spectrometer 3: 0.65
- Channel 10 of spectrometer 3: 0.83
- Channel 20 of spectrometer 3: 0.78
- Channel 32 of spectrometer 3: 0.81

The lenslet array on spectrometer 3 was translated during this measurement so that the laser light can pass through each channel being characterized.

3.6. Loss Due to Beam Splitters

The science beam splitters on the beam combiner table had been characterized previously and found to be close to manufacturer’s specifications. We will use these specified transmission and reflection numbers, since both the accessibility of needed test locations and the time constraints prevented us from carrying out this measurement during the week of August 8. The locations for the intended measurements were described in Figure 7.

At the HeNe frequency, the specified transmission and reflection of the two sets of science beam splitters are 0.52 and 0.48, respectively. The narrow-angle tracker (NAT) coupling beam splitter is specified to induce a throughput transmission on the main path on the order of 0.8.

3.7. Overall System Throughput Performance

The measured values of throughput for the different segments of the NPOI optical train are plotted on Figure 10. Below is a summary of the relative throughput-loss contributions of the different segments of the NPOI optical train, for a “typical” beam path (in this case we choose it to be Astrometric Center station, on beam 2, passing through the science beam splitters A and B with one transmission followed by one reflection, to go into beam Spectrometer 3 (and we choose channel 20 to be a typical channel). All the numbers below are converted to single-pass equivalent throughput:

- Feed system: 0.75
- FDL path: 0.73
- Spectrometer injection optics: 0.46

Beam splitters: $0.5 \times 0.8 = 0.4$ (here we accounted for the loss due to the output ports not used, but folded in the contribution from the other spectrometer where photons will be received and used)

Lenslet array/first fiber path: 0.78

Detector QE*PD: 0.3

We caution here that the detector quantum efficiency (QE) and probability-of-detection (PD) were taken from manufacturer's specifications, and are thus uncertain due to the higher reverse bias we used during normal operations at NPOI.

The total throughput of the system, from multiplying the above numbers together, is 0.024, or 2.4%, close to the estimates obtained by various parties in the past at the HeNe frequency. We note again that this throughput number takes into account the loss due to the un-used ports of one set of beam splitters, but folded-in the photon contribution from the second set of beam splitting which distributes the photons evenly to two spectrometers. The abnormal beamline such as beam 6 will have correspondingly lower total throughput value. Furthermore, these numbers are only for the system performance at the HeNe frequency (633 nm). At the blue end (shorter wavelength) the throughput of the system is known to be much worse from stellar photometry results.

The relative contributions of the front-end and the back-end for a typical NPOI beamline are:

Front-end (feed system and the FDL path including switchyard optics): 0.55

Back-end (beam combiner table optics, unused ports, detector): 0.043

It is clear from the relative magnitude of these two numbers, that for the NPOI optical system the back-end beam combining system (optics, detectors, and un-used ports) contributed more than 10 times as much to the overall throughput loss as the front-end optics (mirrors, plus their propagation paths, and a vacuum windows), even though the front-end mirrors themselves are also under-performing compared to their expected reflectivity. The second-generation NPOI back-end beam combiner currently being designed and developed could potentially yield much better throughput performance, apart from offering better spatial filtering and photometric calibration capabilities.

In stellar observations, since there is seeing-induced throughput loss (the larger curvature of the stellar wavefront means a lower transmission through the pinhole, and also larger loss for any pathlength-dependent transmission), the actual throughput for observing a stellar source should be lower than using the laser source.

4. SUMMARY

In this paper we presented a new approach for systematically characterizing the optical throughput performance of an optical interferometer, as well as the results obtained when applying this approach on the Navy Prototype Optical Interferometer. The first phase of the test gives consistent and repeatable results on throughput, and the interpretation of these results sheds light on the relative contributions of the various segments of the interferometer optics to throughput loss, as well as their physical origins. These results will further guide the design and construction of the second generation beam combining optics for NPOI.

ACKNOWLEDGMENTS

We thank the staff at the NPOI Flagstaff site for the valuable assistance during the data acquisition process of the throughput tests. This research was supported by funding from the Office of Naval Research and from the Oceanographer of the Navy.

REFERENCES

1. J. T. Armstrong, D. Mozurkewich, L.J. Rickard, D.J. Hutter, J.A. Benson, P.F. Bowers, N.M. Elias II, C.A. Hummel, J.J. Johnston, D.F. Buscher, J.H. Clark III, L. Ha, L.C. Ling, N.M. White, and R.S. Simon, "The Navy Prototype Optical Interferometer (NPOI), *Astrophys. J.*, **496**, pp. 550-571 (1998).
2. D. Mozurkewich, "Hybrid Design for a six way beam combiner," in *Amplitude and Intensity Spatial Interferometry II*, J.B. Breckinridge ed., *Proc SPIE* **2200**, 76-80 (1994)
3. X. Zhang, "Throughput characterization of the NPOI optical train: Procedures and first results," *Naval Research Lab Memorandum Report*, NRL/MR/7210-06-8932 (2006)